Electronic Supplementary Material (ESI) for Catalysis Science & Technology.

# $CO_2$ electrochemical reduction at thiolate-modified bulk Au electrodes

*Yuxin Fang, Xun Cheng, John C. Flake,** *and Ye Xu**

Cain Department of Chemical Engineering, Louisiana State University,
Baton Rouge, LA 70803, USA

**Supporting Information**

## S.1 Table of DFT-calculated energetics

**Table S1** DFT-calculated adsorption energies ($\Delta E_{\mathrm{ads}}$, in eV), zero-point energies ($E^{\mathrm{ZPE}}$, in eV), free energies corrections ($\Delta G(T)$, in eV, calculated at $T$=298.15 K), solvation energies ($\Delta E_{\mathrm{solv}}$, in eV), and dipole moments at zero fields ($\mu_0$, in eÅ) for representative species in this study.

| Species | | surface unit cell | $\Delta E_{\mathrm{ads}}$ | $E^{\mathrm{ZPE}}$ | $\Delta G(T)$ | $\Delta E_{\mathrm{solv}}$ | $\mu_0$ |
|---|---|---|---|---|---|---|---|
| $H_2$ | gas phase | | | 0.27 | -0.05 | | |
| $CO_2$ | gas phase | | | 0.31 | -0.30 | | |
| H | Au(111) | (3×3) | -2.08 | 0.13 | 0.13 | | 0.00 |
| | Au(100) | (3×3) | -2.06 | 0.16 | 0.15 | | +0.04 |
| | Au(211) | (4×3) | -2.19 | 0.15 | 0.15 | | +0.02 |
| | Au(563) | 9/layer | -2.16 | 0.16 | 0.15 | | +0.04 |
| CO | Au(111) | (3×3) | -0.13 | 0.18 | 0.07 | -0.1 [a] | -0.10 |
| | Au(100) | (3×3) | -0.16 | 0.17 | 0.06 | -0.1 [a] | -0.07 |
| | Au(211) | (4×3) | -0.37 | 0.17 | 0.06 | -0.1 [a] | -0.11 |
| | Au(563) | 9/layer | -0.50 | 0.18 | 0.07 | -0.1 [a] | -0.09 |
| COOH | Au(111) | (3×3) | -1.17 | 0.61 | 0.47 | -0.25 [a] | +0.25 |
| | Au(100) | (3×3) | -1.15 | 0.61 | 0.47 | -0.25 [a] | +0.30 |
| | Au(211) | (4×3) | -1.42 | 0.61 | 0.48 | -0.25 [a] | +0.31 |
| | Au(563) | 9/layer | -1.50 | 0.61 | 0.47 | -0.25 [a] | +0.33 |
| 2PETt, $C_6H_5(CH_2)_2S$ | Au(111) | (2×2) | -1.38 | 3.96 | 3.71 | | -0.18 |
| | Au(211) | (4×3) | -2.02 | 3.95 | 3.67 | | -0.27 |
| | Au(211) | (2×3) | -1.91 | 3.95 | 3.65 | | -0.23 |
| $(2PETt)_2Au$ | Au(211) | (4×3) | -1.91 [b] | 3.97 [b] | 3.65 [b] | | -0.45 |
| | Au(211) | (3×3) | -1.71 [b] | 3.98 [b] | 3.66 [b] | | -0.37 |
| 2MPAtt, $CH_3CHSCOO$ | Au(111) | (2×2) | +0.19 [c] | 1.83 | 1.60 | | +0.12 |
| | Au(211) | (4×3) | -0.34 [c] | 1.84 | 1.62 | | +0.32 |
| | Au(211) | (2×3) | -0.21 [c] | 1.84 | 1.62 | | +0.21 |
| $(2MPAtt)_2Au$ | Au(211) | (5×3) | -0.40 [b,c] | 1.87 [b] | 1.62 [b] | | +0.31 |
| | Au(211) | (4×3) | -0.37 [b,c] | 1.86 [b] | 1.60 [b] | | +0.22 |

See Computational Methods in the main text for definitions of the terms. Au crystalline facets indicate adsorbed species. ΔG's are calculated at 298.15 K and for gas-phase species, at a pressure of 1 bar.

[a] The solvation energies for adsorbed COOH and CO are taken from Ref. 1.

[b] Energy averaged per thiolate.

[c] With respect to gas-phase $CO_2$ and $CH_3CHS$ because $CH_3CHSCOO$ spontaneously dissociate into the two molecules in gas phase.

## S.2 Additional experimental results

Tafel plots provide general insights into the nature of the possible thermodynamic-limiting, kinetic-limiting and mass transfer-limiting regions. We determined the onset potentials based on the change in slope from the thermodynamically limited region to the kinetic limited region.[2] The onset potential of the cathodic current in $N_2$-purged electrolyte was determined to be the onset potential of the hydrogen evolution reaction (HER). The onset of cathodic current in the $CO_2$-saturated electrolyte provides insights into the thermodynamic preference in $CO_2$ reduction and competing HER with the functionalizing thiols.

The Tafel plots (Fig. S1) were generated using linear sweep voltammetry (LSV) experiments performed in a three-electrode cell with the potential cruised from 0.2 V to -2.0 V vs. Ag/AgCl at 10 mV/s scanning rate. The HER studies was done in a 30 min $N_2$ (Air Liquide, UHP) purged supporting electrolyte (pH=9). For the $CO_2$ (Air Liquide, 99.99%) reduction reaction, $CO_2$ was bubbled into the electrolyte for 30 minutes producing a saturated solution with pH 6.8. All reported potentials (uncompensated resistance corrected) were converted to the RHE scale. The current density was normalized with the geometric area of the gold electrode surface.

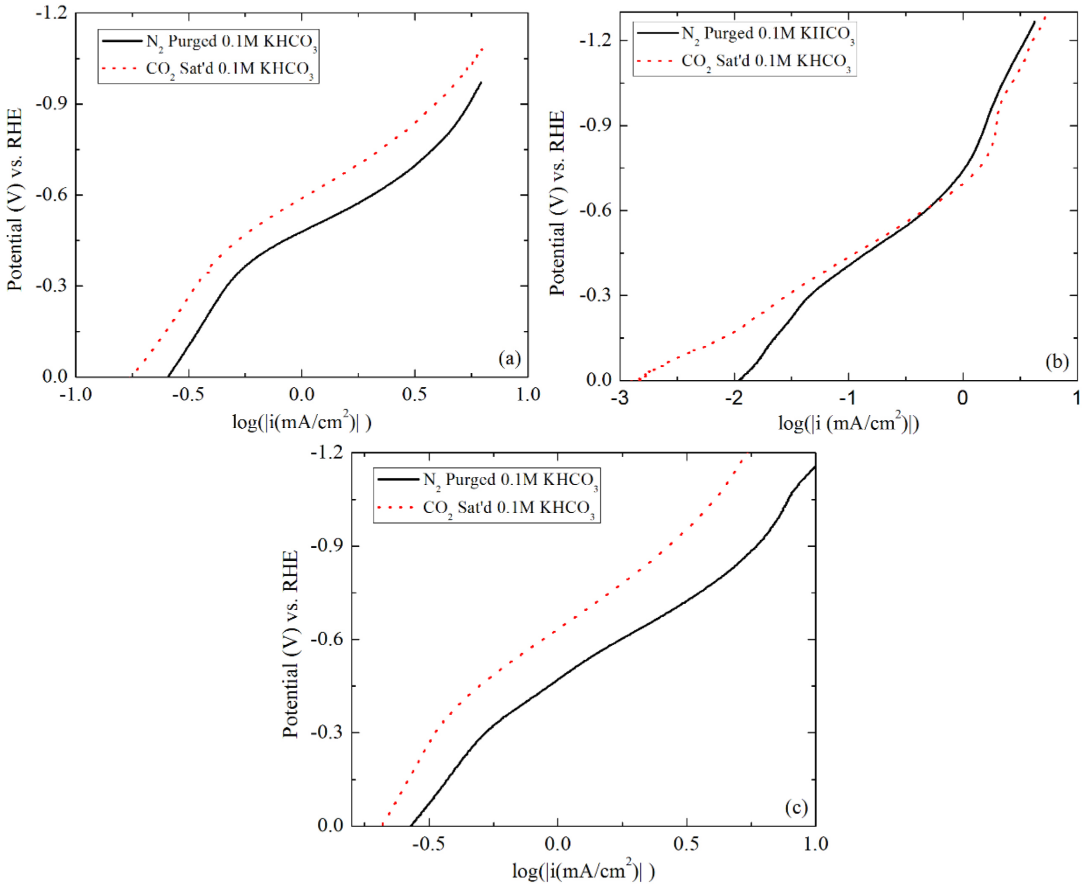

**Fig. S1** Tafel plots of polycrystalline Au electrodes: (a) blank Au; (b) 2-PET-Au; (c) 2-MPA-Au.

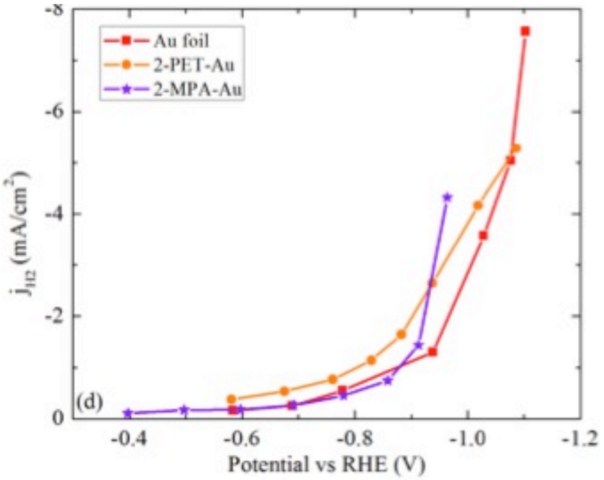

**Fig. S2** The full version of Fig. 3, panel (d).

## S.3 Additional theoretical results

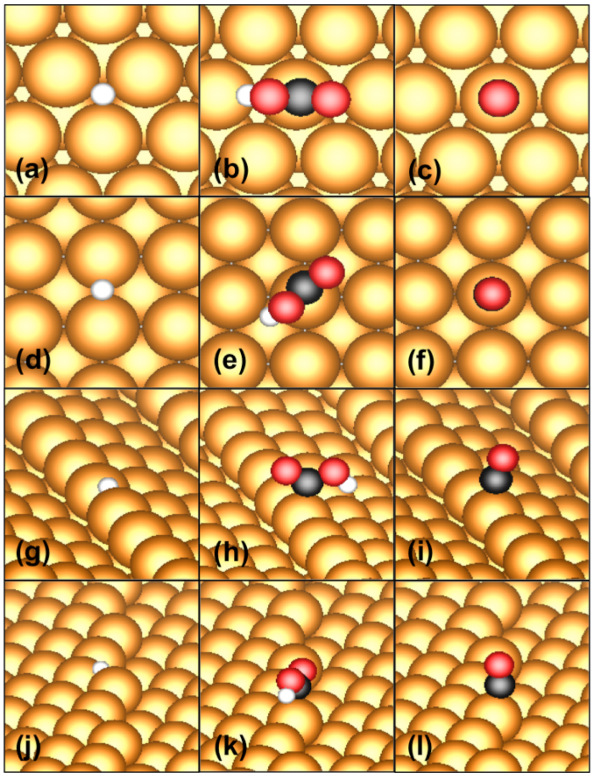

**Fig. S3** DFT-calculated minimum free energy adsorption sites and geometries for H, COOH and CO on (a, b, c) Au(111), (d, e, f) Au(100), (g, h, i) Au(211) and (j, k, l) Au(563), respectively. Yellow, white, black, and red spheres represent Au, H, C, and O atoms, respectively. For clarity, periodic images of adsorbates have been removed.

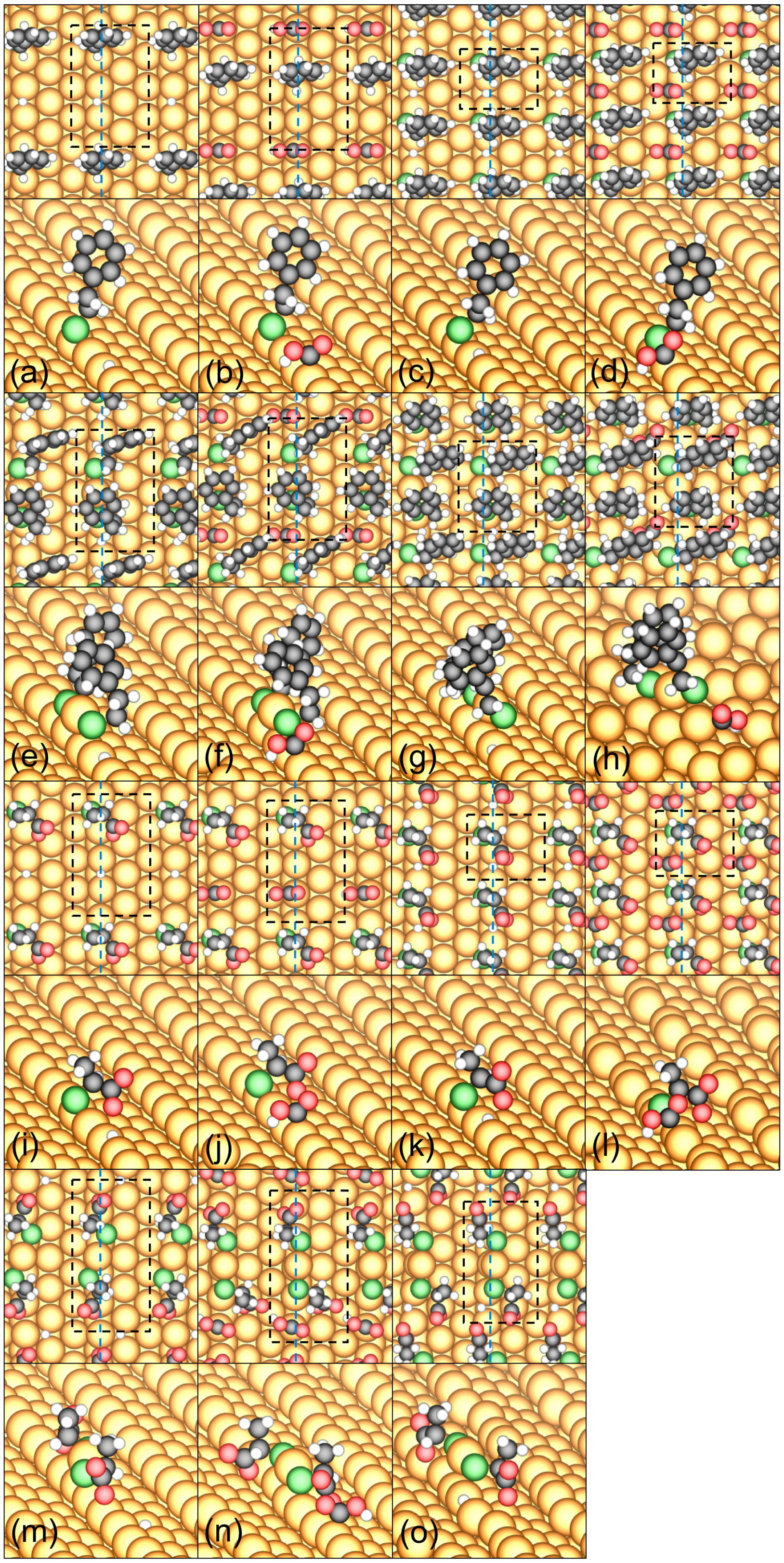
(a)
(b)
(c)
(d)
(e)
(f)
(g)
(h)
(i)
(j)
(k)
(l)
(m)
(n)
(o)

**Fig. S4** Top (top panels) and tilted side (bottom panels) views of DFT-calculated minimum free energy adsorption sites and geometries for 2-PETt co-adsorbed with (a, b) H and COOH on a (4×3) unit cell and co-adsorbed with (c, d) H and COOH on a (2×3) unit cell; $(2\text{-PETt})_2Au$ co-adsorbed with (e, f) H and COOH on a (4×3) unit cell and co-adsorbed with (g, h) H and COOH on a (3×3) unit cell; 2-MPAtt co-adsorbed with (i, j) H and COOH on a (4×3) unit cell and co-adsorbed with (k, l) H and COOH on a (2×3) unit cell; $(2\text{-MPAtt})_2Au$ co-adsorbed with (m, n) H and COOH on a (5×3) unit cell and co-adsorbed with (o) H on a (4×3) unit cell, on step edge of Au(211). Yellow, green, red, black, and white spheres represent Au, S, O, C, and H atoms, respectively. Green and black dashed lines in top views indicate step edge and surface unit cells, respectively. For clarity, periodic images of adsorbates have been removed from the side views.

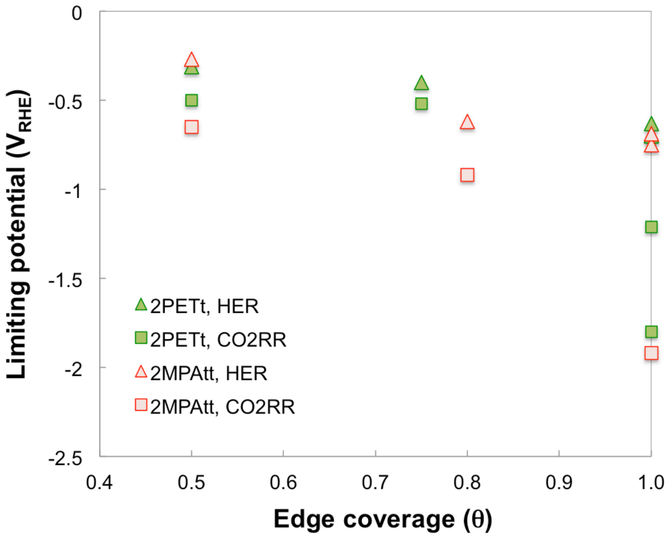

**Fig. S5** Limiting potentials for HER and $CO_2RR$ on various thiolate-functionalized Au(211) step edge plotted against edge coverage, illustrating that H* and COOH* are more destabilized due to 2-MPAtt than to 2-PETt at comparable edge coverages of the thiolates. Values are those listed in Table 4.

## References

1. H. A. Hansen, J. B. Varley, A. A. Peterson and J. K. Nørskov, *J. Phys. Chem. Lett.*, 2013, **4**, 388-392.
2. Y. Yan, X. Ge, Z. Liu, J.-Y. Wang, J.-M. Lee and X. Wang, *Nanoscale*, 2013, **5**, 7768-7771.